Tracking of Extended Objects and Group Targets Using Random Matrices

Michael Feldmann, Dietrich Fränken, *Member, IEEE*, and Wolfgang Koch, *Fellow, IEEE*

***Abstract*—The task of tracking extended objects or (partly) unresolvable group targets raises new challenges for both data association and track maintenance. Due to limited sensor resolution capabilities, group targets (i.e., a number of closely spaced targets moving in a coordinated fashion) may show a similar detection pattern as extended objects, namely a varying number of detections whose spread is determined by both the statistical sensor errors as well as the physical extension of the group or extended object. In both cases, tracking and data association under the "one target–one detection" assumption are no longer applicable. This paper deals with the problem of maintaining a track for an extended object or group target with varying number of detections. Herein, object extension is represented by a symmetric positive definite random matrix. A recently published Bayesian approach to tackling this problem is analyzed and discussed. From there, a new approach is derived that is expected to overcome some of the weaknesses the mentioned Bayesian approach suffers from in certain applications.**

***Index Terms*—Extended targets, formations, group targets, random matrices, sensor resolution, target tracking.**

I. Introduction

KEEPING complex dynamic situations on sea, land, and in the air under surveillance is a challenge, which, in times of network-centric warfare, has to be tackled among other things by the combination of sensor networking and the corresponding sensor data and information fusion procedures. In this context, many tracking applications consider objects to be tracked as point sources [1], i.e., their extension is assumed to be neglectable in comparison with sensor resolution and error. With ever-increasing sensor resolution capabilities, however, this assumption is no longer (or rather less and less) valid, e.g., in short-range applications or for maritime surveillance, where different scattering centers of the observed objects may give rise to several distinct detections varying, from scan to scan, in both number as well as relative origin location. Concerning the fluctuating number of measurements, a similar set of problems arises in the case of closely spaced objects (CSOs), where, depending on the sensor-to-target geometry, limited sensor resolution prevents a successful tracking of (all of) the individual targets [2], [3]. On top of that, hostile fighter aircraft can exploit this surveillance gap by flying in close formation to disguise their actual fighting capacity, where the fluctuating number of measurements and the ambiguities in observation-to-track assignments can entail track instabilities culminating in track loss [3].

Manuscript received December 07, 2009; revised May 14, 2010; accepted December 01, 2010. Date of publication December 20, 2010; date of current version March 09, 2011. The associate editor coordinating the review of this manuscript and approving it for publication was Prof. Andrea Cavallaro.

M. Feldmann and W. Koch are with the Fraunhofer Institute for Communication, Information Processing and Ergonomics FKIE, D-53343 Wachtberg, Germany (e-mail: michael.feldmann@fkie.fraunhofer.de; wolfgang.koch@fkie.fraunhofer.de).

D. Fränken is with EADS Deutschland GmbH, Cassidian Electronics, Data Fusion Algorithms & Software, D-89077 Ulm, Germany (e-mail: dietrich.fraenken@cassidian.com).

Digital Object Identifier 10.1109/TSP.2010.2101064

A. Short Literature Survey

Several suggestions for dealing with this set of problems can be found in literature with varying focus. Authors may concentrate on the data association problem being much more complex than for point targets or on improved estimates for kinematics and/or object extension, all possibly taking into account targets that may be unresolved. A small selection of papers gives a glimpse on the large variety of related aspects.

One example of accounting for possibly unresolved targets is presented in [4], where a sensor resolution model is used to consider additional association hypotheses within an multiple hypothesis tracking (MHT) framework.

Gating methods, usually used to reduce the computational burden of MHT methods, fail to reject non-feasible measurement-to-track assignments in case of CSOs. In order to circumvent this problem, [5] proposes a multiple hypothesis clustering approach relying on a clustering-based data association step, where multiple frame assignment techniques are applied to mitigate the effects of ambivalent clustering possibilities.

Based on the Gaussian mixture probability hypothesis density (GMPHD) filter, [6] identifies possible members of a group of CSOs in a multiple target environment by exploiting the position and velocity components of the individual track files and, in the case of group targets, uses special dynamic models for homogenizing the prediction of group members.

A similar goal is pursued in [7], where the joint dynamic behavior of group targets is emulated by the use of multivariate stochastic differential equations (SDEs). Evaluation of the SDEs is performed by sequential Monte Carlo (SMC) methods.

SMC methods are also used in [8] and [9], where sensor measurements are modeled as a Poisson process with a spatially dependent intensity parameter, which leads to the representation of physical extent as an intensity distribution and herewith avoids the evaluation of explicit data association hypotheses.

The presentation in [10] shows how, for a single point target, possible multiple measurements in presence of detection uncertainty and clutter can be incorporated by means of random finite sets (RFS). Recursive estimation equations are supplemented

with both closed form solutions for the linear Gaussian case as well as SMC implementations for more general ones.

In [11], it is shown that any assumption about an object-dependent spatial distribution of scattering centers can be avoided by means of a combined stochastic and set-theoretic data fusion, where the stochastic part ensures the consideration of statistical sensor errors.

For a more in-depth overview over the variety of related topics, the interested reader may refer to the bibliography [12].

B. Scope of the Paper

In the context of this paper, the recently published Bayesian approach to tracking of extended objects and group targets in [13] seems very promising due to the fact that it tries to estimate both a kinematic state on the one hand and physical extension on the other so that a group of CSOs can be treated as one individual object. While, admittedly, the basic assumption to model the extent by an ellipsoid corresponds with earlier work (see, e.g., [14]–[16]), the novelty of [13] is a joint Bayesian estimation of centroid kinematics and physical extension. Therein, a symmetric positive definite (SPD) random matrix to describe this ellipsoid is the counterpart of a random vector representing the centroid and invokes matrix-variate distributions. The decisive point for tracking of extended objects and CSOs in [13] is the special interpretation of usual sensor data, whereupon each measurement is considered as a measurement of the centroid scattered over object extension. On the one hand, the extent of the object can be *measured* in this way, but, on the other, this assumption implies the neglect of any statistical sensor error. The latter fact has caused some further investigations and developments, preliminary results of that have been published in previous conference papers [17], [18]. Therein as well as in this paper, the focus is on track maintenance, while estimation under uncertain observation-to-track association in possible presence of missed detections and false alarms is considered out of scope.

The presentation in this paper begins with a recapitulation of the Bayesian estimator suggested in [13]. We analyze some of the underlying assumptions and shortly predict its behavior for cases, where these assumptions are not fulfilled. From there, we present the main contributions of this paper starting with the derivation of our new algorithm. We continue with further contributions comprising various aspects with regard to estimation error, moment matching, and confidence regions for the extension estimate of extended objects or groups. It is explained how our new approach can be integrated in an interacting multiple model (IMM). The paper is completed by simulation results comparing both approaches.

II. Bayesian Extended Object Tracking

The recursive estimation of kinematic states based on (associated) measurements is a standard task in many applications. In this paper, we try to estimate kinematic states represented by a random vector $\mathbf{x}_k$ (further on, position and velocity in two or three spatial dimensions, i.e., $\mathbf{x}_k^T = [\mathbf{r}_k^T, \dot{\mathbf{r}}_k^T]$, but acceleration $\ddot{\mathbf{r}}_k^T$ may be added here, of course) using a set of measurements $\mathbf{y}_k^j$ (in the following, position only, i.e., $\mathbf{H} = [\mathbf{I}_d, \mathbf{0}_d]$ with $d = 2$, 3).

As has been stated in the introduction, the Bayesian approach to tracking extended objects and group targets in [13] adds to the kinematic state of the centroid the physical extension represented by a symmetric positive definite (SPD) random matrix $\mathbf{X}_k$ thus considering some ellipsoidal shape. It is assumed that in each scan k there is a random number of n_k independent position measurements

$$\mathbf{y}_k^j = \mathbf{H}\mathbf{x}_k + \mathbf{w}_k^j \tag{1}$$

where $\mathbf{Y}_k := \{\mathbf{y}_k^j\}_{j=1}^{n_k}$ and $\mathcal{Y}_k := \{\mathbf{Y}_\kappa, n_\kappa\}_{\kappa=0}^{k}$ are used to denote the set of the n_k measurements in a particular scan and for the sequence of what is measured scan by scan, respectively. With statistical sensor error assumed to be neglectable and the extension thus dominating the spread of measurements, the noise $\mathbf{w}_k^j$ according to [13] is assumed to be a zero mean normally distributed random vector with variance $\mathbf{X}_k$. With this, the likelihood to measure the set $\mathbf{Y}_k$ given both kinematic state and extension as well as the number of measurements, reads

$$p(\mathbf{Y}_k|n_k, \mathbf{x}_k, \mathbf{X}_k) = \prod_{j=1}^{n_k} \mathcal{N}\left(\mathbf{y}_k^j; \mathbf{H}\mathbf{x}_k, \mathbf{X}_k\right) \tag{2}$$

where $\mathcal{N}(\mathbf{x}; \boldsymbol{\mu}, \boldsymbol{\Sigma})$ denotes the *normal density* with mean $\boldsymbol{\mu}$ and variance $\boldsymbol{\Sigma}$. Introducing the mean measurement and the measurement spread

$$\overline{\mathbf{y}}_k = \frac{1}{n_k}\sum_{j=1}^{n_k} \mathbf{y}_k^j, \quad \overline{\mathbf{Y}}_k = \sum_{j=1}^{n_k} \left(\mathbf{y}_k^j - \overline{\mathbf{y}}_k\right)\left(\mathbf{y}_k^j - \overline{\mathbf{y}}_k\right)^T \tag{3}$$

(2) can be written as

$$p(\mathbf{Y}_k|n_k, \mathbf{x}_k, \mathbf{X}_k) \propto \mathcal{N}(\overline{\mathbf{y}}_k; \mathbf{H}\mathbf{x}_k, \mathbf{X}_k/n_k) \times \mathcal{W}(\overline{\mathbf{Y}}_k; n_k - 1, \mathbf{X}_k) \tag{4}$$

where

$$\mathcal{W}(\mathbf{X}; m, \mathbf{C}) = \frac{|\mathbf{X}|^{\frac{m-d-1}{2}}}{2^{\frac{md}{2}}\,\Gamma_d\left(\frac{m}{2}\right)|\mathbf{C}|^{\frac{m}{2}}}\mathrm{etr}\left(-\frac{1}{2}\mathbf{X}\mathbf{C}^{-1}\right) \tag{5}$$

with $m \geq d$ denotes the *Wishart density* [19] of a d-dimensional SPD random matrix $\mathbf{X}$ with expected SPD matrix $m\mathbf{C}$; $\mathrm{etr}(\cdot)$ is an abbreviation for $\exp(\mathrm{tr}(\cdot))$ and $\Gamma_d(\cdot)$ is the multivariate gamma function.

In [13], the concept of *conjugate priors*—the very same concept that constitutes one possible way of deriving the well-known Kalman filter equations for point source tracking—is applied to this measurement equation for deriving update equations and then complemented with an evaluation of the *Chapman-Kolmogorov* theorem for obtaining a recursive Bayesian estimation cycle. We only summarize the results here, additionally necessary assumptions and detailed derivation steps can be found in the original publication.

The resulting estimator is based on specific product forms of prior and posterior densities. In particular, the posterior (with corresponding expressions for the prior) is factored as

$$p(\mathbf{x}_k, \mathbf{X}_k|\mathcal{Y}_k) = p(\mathbf{x}_k|\mathbf{X}_k, \mathcal{Y}_k)p(\mathbf{X}_k|\mathcal{Y}_k). \tag{6}$$

Within this product, the matrix-variate density is given by

$$p(\mathbf{X}_k|\boldsymbol{\mathcal{Y}}_k) = \mathcal{IW}(\mathbf{X}_k; \nu_{k|k}, \widetilde{\mathbf{X}}_{k|k}) \tag{7}$$

where the *inverse Wishart density* [19] with parameterization

$$\mathcal{IW}(\mathbf{X}; m, \mathbf{C}) = \frac{|\mathbf{C}|^{\frac{m}{2}}}{2^{\frac{md}{2}}\Gamma_d\left(\frac{m}{2}\right)|\mathbf{X}|^{\frac{m+d+1}{2}}}\operatorname{etr}\left(-\frac{1}{2}\mathbf{C}\mathbf{X}^{-1}\right) \tag{8}$$

possesses the expected SPD matrix $\mathbf{C}/(m-d-1)$ for $m-d-1>0$. The vector-variate density reads

$$p(\mathbf{x}_k|\mathbf{X}_k, \boldsymbol{\mathcal{Y}}_k) = \mathcal{N}(\mathbf{x}_k; \mathbf{x}_{k|k}, \widetilde{\mathbf{P}}_{k|k} \otimes \mathbf{X}_k). \tag{9}$$

Herein, $\otimes$ denotes the *Kronecker product* [20] that, e.g., yields

$$\begin{bmatrix} \widetilde{p}_{11} & \widetilde{p}_{21} \\ \widetilde{p}_{21} & \widetilde{p}_{22} \end{bmatrix} \otimes \mathbf{X}_k = \begin{bmatrix} \widetilde{p}_{11}\mathbf{X}_k & \widetilde{p}_{21}\mathbf{X}_k \\ \widetilde{p}_{21}\mathbf{X}_k & \widetilde{p}_{22}\mathbf{X}_k \end{bmatrix} \tag{10}$$

and

$$\mathbf{H} = [\mathbf{I}_d, \mathbf{0}_d] = \widetilde{\mathbf{H}} \otimes \mathbf{I}_d \quad \text{with} \quad \widetilde{\mathbf{H}} = [1, 0]. \tag{11}$$

Based on the given forms of prior and posterior densities, the update equations of the estimator comprise

$$\mathbf{S}_{k|k-1} = \widetilde{S}_{k|k-1}\mathbf{X}_k, \quad \widetilde{S}_{k|k-1} = \widetilde{\mathbf{H}}\widetilde{\mathbf{P}}_{k|k-1}\widetilde{\mathbf{H}}^T + \frac{1}{n_k} \tag{12}$$

and hence a scalar innovation variance $\widetilde{S}_{k|k-1}$ as well as

$$\mathbf{K}_{k|k-1} = \widetilde{\mathbf{K}}_{k|k-1} \otimes \mathbf{I}_d, \quad \widetilde{\mathbf{K}}_{k|k-1} = \widetilde{\mathbf{P}}_{k|k-1}\widetilde{\mathbf{H}}^T\widetilde{S}^{-1}_{k|k-1} \tag{13}$$

and thus a gain being independent of $\mathbf{X}_k$. The update of the kinematic parameters is performed according to

$$\mathbf{x}_{k|k} = \mathbf{x}_{k|k-1} + (\widetilde{\mathbf{K}}_{k|k-1} \otimes \mathbf{I}_d)(\overline{\mathbf{y}}_k - \mathbf{H}\mathbf{x}_{k|k-1}) \tag{14}$$

$$\widetilde{\mathbf{P}}_{k|k} = \widetilde{\mathbf{P}}_{k|k-1} - \widetilde{\mathbf{K}}_{k|k-1}\widetilde{S}_{k|k-1}\widetilde{\mathbf{K}}^T_{k|k-1}. \tag{15}$$

The update equations for the extension parameters read

$$\nu_{k|k} = \nu_{k|k-1} + n_k \tag{16}$$

as well as

$$\widetilde{\mathbf{X}}_{k|k} = \widetilde{\mathbf{X}}_{k|k-1} + \widetilde{S}^{-1}_{k|k-1}\mathbf{N}_{k|k-1} + \overline{\mathbf{Y}}_k \tag{17}$$

with

$$\mathbf{N}_{k|k-1} = (\overline{\mathbf{y}}_k - \mathbf{H}\mathbf{x}_{k|k-1})(\overline{\mathbf{y}}_k - \mathbf{H}\mathbf{x}_{k|k-1})^T. \tag{18}$$

It should be noted that the parameters of the density $p(\mathbf{x}_k, \mathbf{X}_k|\boldsymbol{\mathcal{Y}}_k)$ do not directly constitute all sought quantities as, e.g., the extension estimate or the error variance of the kinematic estimate. The former can be immediately deduced from $p(\mathbf{X}_k|\boldsymbol{\mathcal{Y}}_k) = \mathcal{IW}(\mathbf{X}_k; \nu_{k|k}, \widetilde{\mathbf{X}}_{k|k})$ as

$$\mathbf{X}_{k|k} := E[\mathbf{X}_k|\boldsymbol{\mathcal{Y}}_k] = \frac{\widetilde{\mathbf{X}}_{k|k}}{\nu_{k|k} - d - 1}. \tag{19}$$

The latter (not being $\widetilde{\mathbf{P}}_{k|k}$) has to be obtained from the marginal density $p(\mathbf{x}_k|\boldsymbol{\mathcal{Y}}_k) = \int p(\mathbf{x}_k, \mathbf{X}_k|\boldsymbol{\mathcal{Y}}_k)\mathrm{d}\mathbf{X}_k$ that, after some tedious computations, turns out to be

$$p(\mathbf{x}_k|\boldsymbol{\mathcal{Y}}_k) = \mathcal{T}\left(\mathbf{x}_k; \widetilde{\nu}_{k|k}, \mathbf{x}_{k|k}, \widetilde{\mathbf{P}}_{k|k} \otimes (\widetilde{\mathbf{X}}_{k|k}/\widetilde{\nu}_{k|k})\right) \tag{20}$$

with $\widetilde{\nu}_{k|k} = \nu_{k|k} + s - sd > 0$, where s is 2 if the state consists of position and velocity alone (3 if acceleration is also considered) and

$$\mathcal{T}(\mathbf{x}; m, \boldsymbol{\mu}, \mathbf{C}) = \frac{\Gamma\left(\frac{m+p}{2}\right)}{(m\pi)^{\frac{p}{2}}\Gamma\left(\frac{m}{2}\right)|\mathbf{C}|^{\frac{1}{2}}} \times \left(1 + \frac{1}{m}(\mathbf{x}-\boldsymbol{\mu})^T\mathbf{C}^{-1}(\mathbf{x}-\boldsymbol{\mu})\right)^{-\frac{m+p}{2}} \tag{21}$$

is the *Student-t density* [21] of a p-dimensional random vector $\mathbf{x}$ with mean $\boldsymbol{\mu}$ and variance $\frac{m}{m-2}\mathbf{C}$ for $m>2$ and a p-dimensional SPD matrix $\mathbf{C}$ (with $p = sd$). With this, $\mathbf{x}_{k|k}$ is the kinematic estimate $E[\mathbf{x}_k|\boldsymbol{\mathcal{Y}}_k] = \int \mathbf{x}_k p(\mathbf{x}_k|\boldsymbol{\mathcal{Y}}_k)\mathrm{d}\mathbf{x}_k$ leading to the error variance

$$E\left[(\mathbf{x}_k - \mathbf{x}_{k|k})(\mathbf{x}_k - \mathbf{x}_{k|k})^T|\boldsymbol{\mathcal{Y}}_k\right] = (\widetilde{\mathbf{P}}_{k|k} \otimes \widetilde{\mathbf{X}}_{k|k})/(\widetilde{\nu}_{k|k} - 2). \tag{22}$$

Finally, the prediction equations of the estimator as proposed in [13] read

$$\mathbf{x}_{k|k-1} = \mathbf{F}\mathbf{x}_{k-1|k-1} \tag{23}$$

$$\widetilde{\mathbf{P}}_{k|k-1} = \widetilde{\mathbf{F}}\widetilde{\mathbf{P}}_{k-1|k-1}\widetilde{\mathbf{F}}^T + \widetilde{\mathbf{Q}} \tag{24}$$

and

$$\widetilde{\mathbf{X}}_{k|k-1} = \frac{\nu_{k|k-1} - d - 1}{\nu_{k-1|k-1} - d - 1}\widetilde{\mathbf{X}}_{k-1|k-1} \tag{25}$$

as well as

$$\nu_{k|k-1} = \exp(-T/\tau)\nu_{k-1|k-1} \tag{26}$$

with τ denoting some time constant related to the agility with which the object may change its extension over time and T being the prediction time interval.

At this point, it is needed to mention some special features of the estimator derived in [13]. First of all, there is an almost fixed (up to a scalar factor) coupling between the estimated extension $\mathbf{X}_{k|k}$ and the mean squared position estimation error because, with a $\widetilde{\mathbf{P}}_{k|k}$ as in (10), the error variance of the position estimate due to (22) reads

$$E\left[(\mathbf{r}_k - \mathbf{r}_{k|k})(\mathbf{r}_k - \mathbf{r}_{k|k})^T|\boldsymbol{\mathcal{Y}}_k\right] = \frac{\widetilde{p}_{11}}{\widetilde{\nu}_{k|k} - 2}\widetilde{\mathbf{X}}_{k|k}. \tag{27}$$

Moreover, although both the prediction (23), (24) and the update (14), (15) of the kinematic state look similar to that of a Kalman filter, the parameter $\widetilde{\mathbf{P}}_{k|\ell}$ therein behaves as the solution of the tracking problem in one spatial dimension with $\widetilde{\mathbf{Q}}$ being of the same reduced dimension. Consequently, an equal Kalman gain is effective in each spatial dimension, independently of the actual sensor performance. Finally, (24) implies that the effective process noise $\widetilde{\mathbf{Q}} \otimes \mathbf{X}_k$ driving the centroid kinematics depends

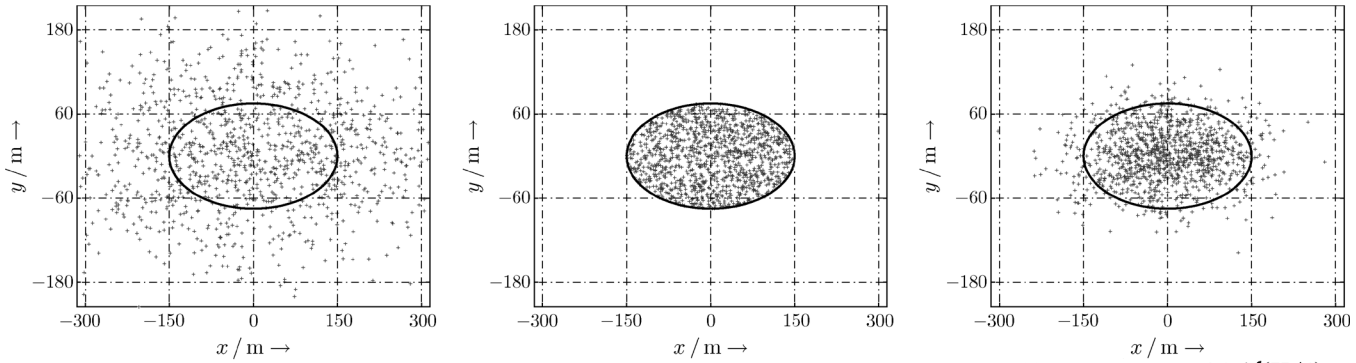

(a) Measurement model $\mathcal{N}(\mathbf{X})$ **(b)** Measurement model $\mathcal{U}(\mathbf{X})$ **(c)** Measurement model $\mathcal{N}(\mathbf{X}/4)$

Fig. 1. Spread of 1200 measurements based on an SPD matrix $\mathbf{X} = \mathrm{diag}((300\,\mathrm{m}/2)^2, (150\,\mathrm{m}/2)^2)$ with (a) $\mathbf{y} \sim \mathcal{N}(\mathbf{0}, \mathbf{X})$, (b) $\mathbf{y} \sim \mathcal{U}(\mathbf{0}, \mathbf{X}) = \pi^{-1}|\mathbf{X}|^{-1/2}$ for $\mathbf{y}^T\mathbf{X}^{-1}\mathbf{y} \leq 1 \Longrightarrow \mathrm{Var}[\mathbf{y}] = \mathbf{X}/4$, (c) $\mathbf{y} \sim \mathcal{N}(\mathbf{0}, \mathbf{X}/4)$.

on the size of the object in a very specific way, which means that larger objects become more reactive (see [13] for arguments that may justify this assumption).

III. A Different Approach

The closing remarks of the previous section can have significant impact on the behavior of the estimator of [13] due to the fact that it, in presence of sensor error, effectively estimates extension *plus* sensor error. With increasing sensor error, it can be expected to overestimate the object size and herewith to assume a too large agility of the tracked object, which, in consequence, would lead to a more than proportionally increased centroid estimation error according to (22) and (27).

We thus expect some degraded estimation performance with respect to the centroid kinematics in those cases, where sensor errors cannot be neglected any more when compared to object extension, i.e., where both are within the same order of magnitude. In order to compensate for this effect, it is not sufficient to let the original approach estimate extension plus sensor error and merely subtract the sensor error contribution afterwards in order to obtain a true *extension-only* estimate. Apart from that, there is no guarantee that the resulting matrix would remain positive definite in any case and, finally, it is unclear how such a procedure would work for multiple sensors with different sensor errors.

A. Adjustment of the Measurement Likelihood Function

Explicitly accounting for possible sensor errors, we use, as an approximation to the true behavior, (1) with noise $\mathbf{w}_k^j$ being normally distributed with variance $z\mathbf{X}_k + \mathbf{R}$ and thus write

$$p(\mathbf{Y}_k|n_k, \mathbf{x}_k, \mathbf{X}_k) = \prod_{j=1}^{n_k} \mathcal{N}\left(\mathbf{y}_k^j; \mathbf{H}\mathbf{x}_k, z\mathbf{X}_k + \mathbf{R}\right). \quad (28)$$

In addition to the sensor error covariance matrix $\mathbf{R}$, we have added a scaling factor z to the spread contribution of the object extension. The latter is mostly of technical interest only and enables us to account for a difference between an assumed normal spread contribution of the extension and a possibly more realistic assumption like, e.g., a uniform distribution of varying scattering centers over an object of finite extent as illustrated in Fig. 1. Of course, such a factor can also be integrated into the original Bayesian approach of [13].

Now, it appears that, for the likelihood in (28), no conjugate prior can be found that is both independent of $\mathbf{R}$ and analytically traceable. Thus, some careful approximations are necessary.

B. Improved Measurement Update

If the object extension $\mathbf{X}_k$ were non-random and known and thus not part of the estimation problem, and if, in addition, the prior density were normal according to $p(\mathbf{x}_k|\boldsymbol{\mathcal{Y}}_{k-1}) = \mathcal{N}(\mathbf{x}_k; \mathbf{x}_{k|k-1}, \mathbf{P}_{k|k-1})$, the updated estimate of the centroid kinematics could immediately be determined by using standard Kalman filter update equations with suitable substitutions of terms. In the following, we will use this procedure while replacing $\mathbf{X}_k$ with its approximation $\mathbf{X}_{k|k-1}$ where needed. In detail, we propose to perform the update, herein merely ignoring the uncertainty coming with the predicted estimate, according to

$$\mathbf{x}_{k|k} = \mathbf{x}_{k|k-1} + \mathbf{K}_{k|k-1}(\overline{\mathbf{y}}_k - \mathbf{H}\mathbf{x}_{k|k-1}) \quad (29)$$

$$\mathbf{P}_{k|k} = \mathbf{P}_{k|k-1} - \mathbf{K}_{k|k-1}\mathbf{S}_{k|k-1}\mathbf{K}_{k|k-1}^T \quad (30)$$

with

$$\mathbf{S}_{k|k-1} = \mathbf{H}\mathbf{P}_{k|k-1}\mathbf{H}^T + \frac{\mathbf{Y}_{k|k-1}}{n_k} \quad (31)$$

being an approximation of the true innovation covariance,

$$\mathbf{K}_{k|k-1} = \mathbf{P}_{k|k-1}\mathbf{H}^T\mathbf{S}_{k|k-1}^{-1} \quad (32)$$

denoting the corresponding gain, and

$$\mathbf{Y}_{k|k-1} = z\mathbf{X}_{k|k-1} + \mathbf{R} \quad (33)$$

indicating the predicted variance of a single measurement. This proposal may be interpreted as approximating the posterior of the kinematic state conditioned on the extension by the respective (in fact unknown) marginalized density that in turn is assumed to be close to a normal density again, i.e.,

$$p(\mathbf{x}_k|\mathbf{X}_k, \boldsymbol{\mathcal{Y}}_k) \approx p(\mathbf{x}_k|\boldsymbol{\mathcal{Y}}_k) \approx \mathcal{N}(\mathbf{x}_k; \mathbf{x}_{k|k}, \mathbf{P}_{k|k}). \quad (34)$$

Note that (31) may be seen as a variant of (12), but now having a kinematic state prediction error with a full set of parameters

and an additional contribution to $\mathbf{S}_{k|k-1}$ induced by the sensor error.

As an update of the estimate $\mathbf{X}_{k|k}$ (rather than the parameter $\widetilde{\mathbf{X}}_{k|k}$), the predicted extension $\mathbf{X}_{k|k-1}$, the term $\mathbf{N}_{k|k-1}$ of (18) and the measurement spread $\overline{\mathbf{Y}}_k$ of (3) are summed up being weighted by scalar or matrix-valued factors. To this end, we again consider the limiting case of a non-random $\mathbf{X}_k$ and a prediction $\mathbf{X}_{k|k-1}$ being (about) the same. More precisely, we note that the quantity $\mathbf{N}_{k|k-1}$ obeys

$$E[\mathbf{N}_{k|k-1}|\mathcal{Y}_{k-1}, \mathbf{X}_k = \mathbf{X}_{k|k-1}] = \mathbf{S}_{k|k-1} \tag{35}$$

with $\mathbf{S}_{k|k-1}$ as given in (31) and, similarly,

$$E[\overline{\mathbf{Y}}_k|\mathcal{Y}_{k-1}, \mathbf{X}_k = \mathbf{X}_{k|k-1}] = (n_k - 1)\mathbf{Y}_{k|k-1}. \tag{36}$$

By an appropriate (matrix-valued) scaling, we generate some quantities $\widehat{\mathbf{N}}_{k|k-1}$ and $\widehat{\mathbf{Y}}_{k|k-1}$ that both yield conditional expected matrices being proportional to $\mathbf{X}_k = \mathbf{X}_{k|k-1}$ while preserving the symmetric positive (semi-)definite structure. This is done by computing some square roots (e.g., via Cholesky factorization) of the matrices $\mathbf{X}_{k|k-1}$, $\mathbf{S}_{k|k-1}$, and $\mathbf{Y}_{k|k-1}$ that obey

$$\mathbf{X}_{k|k-1} = \mathbf{X}_{k|k-1}^{1/2}\left(\mathbf{X}_{k|k-1}^{1/2}\right)^T \tag{37}$$

etc., and by setting, in view of (35) and (36) above,

$$\widehat{\mathbf{N}}_{k|k-1} = \mathbf{X}_{k|k-1}^{1/2}\mathbf{S}_{k|k-1}^{-1/2}\mathbf{N}_{k|k-1}\left(\mathbf{S}_{k|k-1}^{-1/2}\right)^T\left(\mathbf{X}_{k|k-1}^{1/2}\right)^T \tag{38}$$

$$\widehat{\mathbf{Y}}_{k|k-1} = \mathbf{X}_{k|k-1}^{1/2}\mathbf{Y}_{k|k-1}^{-1/2}\overline{\mathbf{Y}}_k\left(\mathbf{Y}_{k|k-1}^{-1/2}\right)^T\left(\mathbf{X}_{k|k-1}^{1/2}\right)^T. \tag{39}$$

Hence, the updated extension estimate

$$\mathbf{X}_{k|k} = \frac{1}{\alpha_{k|k}}(\alpha_{k|k-1}\mathbf{X}_{k|k-1} + \widehat{\mathbf{N}}_{k|k-1} + \widehat{\mathbf{Y}}_{k|k-1}) \tag{40}$$

yields the conditional expected matrix $\mathbf{X}_k = \mathbf{X}_{k|k-1}$ again, if the parameters $\alpha_{k|k-1}$ and $\alpha_{k|k}$ are related via

$$\alpha_{k|k} = \alpha_{k|k-1} + n_k. \tag{41}$$

Note the similarity between the choice (40) and (17) as well as between (41) and (16) because it reveals our underlying assumption that the marginalized prior density of the extension is an inverse Wishart density and that the corresponding (also in fact unknown) posterior is again of the same form, i.e.,

$$p(\mathbf{X}_k|\mathcal{Y}_k) \approx \mathcal{IW}(\mathbf{X}_k; \nu_{k|k}, \alpha_{k|k}\mathbf{X}_{k|k}) \tag{42}$$

with $\alpha_{k|k} = \nu_{k|k} - d - 1$. Finally, we would like to point out that, despite all our approximations in the measurement update step, $\mathbf{S}_{k|k-1}$ and $\widehat{\mathbf{N}}_{k|k-1}$ provide for the interdependency between kinematics and extension estimation.

C. Improved Time Update

With the assumed (approximate) independence between the estimates for centroid kinematics and extension expressed in (34) and further assuming independent dynamic models for both of them, the standard Kalman filter prediction equations

$$\mathbf{x}_{k|k-1} = \mathbf{F}\mathbf{x}_{k-1|k-1} \tag{43}$$

$$\mathbf{P}_{k|k-1} = \mathbf{F}\mathbf{P}_{k-1|k-1}\mathbf{F}^T + \mathbf{Q} \tag{44}$$

with process noise variance $\mathbf{Q}$ now being of full dimension are applicable while, owing to the assumption that the extension does not tend to change over time, it is suggested to use

$$\mathbf{X}_{k|k-1} = \mathbf{X}_{k-1|k-1}. \tag{45}$$

Now, we will see later on that the variance of the extension estimate is approximately proportional to $1/(\alpha_{k|k} - 2)$ for both very large $\alpha_{k|k}$ as well as values of $\alpha_{k|k}$ close to 2, where $\alpha_{k|k} > 2$ is required to hold. In view of this, we suggest to assume an exponential increase of variance over time according to

$$\alpha_{k|k-1} = 2 + \exp(-T/\tau)(\alpha_{k-1|k-1} - 2). \tag{46}$$

IV. Characteristics of the Extension Estimate

The two approaches recalled in the previous sections share one common feature, namely the fact that the marginal for the extension is an inverse Wishart density. In the following, we will focus on this matrix-valued density and discuss some related aspects.

A. Estimation Error

Let $\hat{\mathbf{X}}_k$ denote any estimate for the symmetric positive definite matrix $\mathbf{X}_k$. The mean square error (MSE) $\hat{e}_{k|k}$ of this estimate is computed by summing up the mean square errors obtained for each element of $\hat{\mathbf{X}}_k$ with respect to $\mathbf{X}_k$. As both $\hat{\mathbf{X}}_k$ and $\mathbf{X}_k$ are SPD matrices, this error can be written as

$$\hat{e}_{k|k} = \mathrm{tr}E\left[(\hat{\mathbf{X}}_k - \mathbf{X}_k)^2|\mathcal{Y}_k\right]. \tag{47}$$

As has been shown in [18], this expression becomes minimal for $\hat{\mathbf{X}}_k = \mathbf{X}_{k|k}$. In other words, the conditional mean

$$E[\mathbf{X}_k|\mathcal{Y}_k] = \mathbf{X}_{k|k} = \frac{\widetilde{\mathbf{X}}_{k|k}}{\alpha_{k|k}} \quad \text{with} \quad \alpha_{k|k} = \nu_{k|k} - d - 1 \tag{48}$$

is the MMSE estimator (just as it is in the vector-variate case) and its squared estimation error $e_{k|k}$ can be computed from the variance

$$\mathrm{Var}[\mathbf{X}_k|\mathcal{Y}_k] := E\left[\mathbf{X}_k^2|\mathcal{Y}_k\right] - \mathbf{X}_{k|k}^2 \tag{49}$$

according to $e_{k|k} = \mathrm{tr}\mathrm{Var}[\mathbf{X}_k|\mathcal{Y}_k]$. For an SPD random matrix following an inverse Wishart distribution (42), the variance $\mathbf{V}_{k|k} := \mathrm{Var}[\mathbf{X}_k|\mathcal{Y}_k]$ is given by[1]

$$\mathbf{V}_{k|k} = \frac{\alpha_{k|k}(\mathrm{tr}\mathbf{X}_{k|k})\mathbf{X}_{k|k} + (\alpha_{k|k} + 2)\mathbf{X}_{k|k}^2}{(\alpha_{k|k} + 1)(\alpha_{k|k} - 2)} \tag{50}$$

for $\alpha_{k|k} > 2$.

B. Moment Matching

With the preceding results concerning an estimation error, it becomes apparent that moment matching, i.e., the process

[1]Let $\mathbf{X} \sim \mathcal{IW}(m, \mathbf{C})$ according to the parameterization (8), then it yields $E[\mathbf{X}^2] = (\mathrm{tr}(\mathbf{C})\mathbf{C} + (m - d - 1)\mathbf{C}^2)/((m - d)(m - d - 1)(m - d - 3))$ for $m - d > 3$ (see [19]).

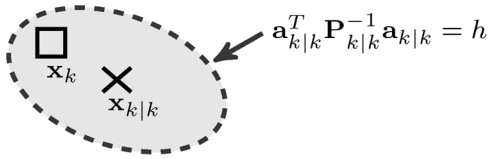

Fig. 2. Confidence region for a normally distributed random vector (position part only). Shown are the estimated position ($\times$) and the true position ($\square$) as well as the border (---) of the confidence region.

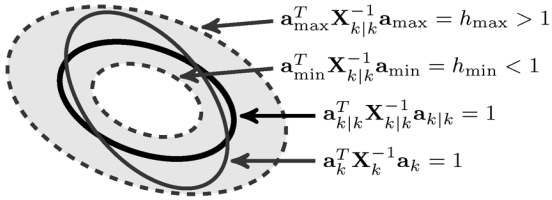

Fig. 3. Confidence region for an SPD random matrix having an inverse Wishart distribution. Shown are the estimated extension (black) and the true extension (gray) as well as the inner and outer border (---) of the confidence region.

of determining the parameters of the inverse Wishart distribution from given first and second order moments, leaves only the single free parameter $\alpha_{k|k}$ once the expected matrix $\mathbf{X}_{k|k}$ has been fixed. Hence, it cannot be expected in general to be able to fulfill (50) completely for any given $\mathbf{V}_{k|k}$. However, from $e_{k|k} = \mathrm{tr}\mathrm{Var}[\mathbf{X}_k|\boldsymbol{\mathcal{Y}}_k]$, a quadratic equation $e_{k|k}\alpha_{k|k}^2 - p_{k|k}\alpha_{k|k} - q_{k|k} = 0$ and next the solution

$$\alpha_{k|k} = \frac{p_{k|k} + \sqrt{p_{k|k}^2 + 4e_{k|k}q_{k|k}}}{2e_{k|k}} \tag{51}$$

with

$$p_{k|k} = e_{k|k} + (\mathrm{tr}\mathbf{X}_{k|k})^2 + \mathrm{tr}\left(\mathbf{X}_{k|k}^2\right) > e_{k|k} \tag{52}$$

$$q_{k|k} = 2\left(e_{k|k} + \mathrm{tr}\left(\mathbf{X}_{k|k}^2\right)\right) > 2e_{k|k} \tag{53}$$

can be derived. Note that in (51) the negative of the square root cannot be used instead as this would yield some negative $\alpha_{k|k}$. On the other hand, the selected sign obviously ensures $\alpha_{k|k} > 2$ and thus a valid solution.

C. Confidence Regions

In addition to a good estimate, a useful estimator is also required to deliver a reliable quality measure, typically in form of the corresponding MSE. For the kinematics estimate $\mathbf{x}_{k|k}$, this MSE is given by $\mathrm{tr}\mathrm{Var}[\mathbf{x}_k|\boldsymbol{\mathcal{Y}}_k]$ and, as shown above, for the extension estimate $\mathbf{X}_{k|k}$ likewise by $\mathrm{tr}\mathrm{Var}[\mathbf{X}_k|\boldsymbol{\mathcal{Y}}_k]$. More detailed information than the respective numbers alone can be envisioned by displaying certain confidence regions. For the kinematics estimate, this is rather standard. With $\mathrm{Var}[\mathbf{x}_k|\boldsymbol{\mathcal{Y}}_k] = \mathbf{P}_{k|k}$ and a prescribed confidence value c, a height level $h = h(c)$ is computed such that, with probability c, the *normalized error squared*

$$d_{k|k} = (\mathbf{x}_{k|k} - \mathbf{x}_k)^T \mathbf{P}_{k|k}^{-1} (\mathbf{x}_{k|k} - \mathbf{x}_k) \tag{54}$$

is not larger than h, i.e., the true value $\mathbf{x}_k$ will lie within the bordering ellipse consisting of the values $\mathbf{c}_{k|k}$ that obey $\mathbf{a}_{k|k}^T \mathbf{P}_{k|k}^{-1} \mathbf{a}_{k|k} = h$ with $\mathbf{a}_{k|k} := \mathbf{c}_{k|k} - \mathbf{x}_{k|k}$ as shown in Fig. 2. Here, $h(c)$ can be determined numerically under normality assumptions because $d_{k|k}$ then possesses a χ^2-distribution.

Now, we will discuss how to envision a confidence region for the extension estimate. We start with the observation that, although $\mathrm{Var}[\mathbf{X}_k|\boldsymbol{\mathcal{Y}}_k]$ is again a symmetric positive definite matrix, the meaning of any ellipse defined by this matrix remains unclear. But, an ellipse defined by

$$\mathbf{a}_{k|k}^T \mathbf{X}_{k|k}^{-1} \mathbf{a}_{k|k} = 1 \tag{55}$$

can directly be interpreted as the estimated extension as depicted in Fig. 3. In view of the chosen interpretation, the true extension would be given by

$$\mathbf{a}_k^T \mathbf{X}_k^{-1} \mathbf{a}_k = 1. \tag{56}$$

Hence, our goal must be to find a region such that we get with prescribed probability c an $\mathbf{X}_k$, where the complete set of points $\mathbf{a}_k$ obeying (56) for this $\mathbf{X}_k$ remains in that region. Herein, we note from Fig. 3 that such an $\mathbf{X}_k$ can yield both a different orientation as well as a different ratio of semi-axes in comparison with what results from the estimated $\mathbf{X}_{k|k}$.

At this point, we propose to use as borders of the confidence region two different height lines determined by the estimate as also depicted in Fig. 3. More precisely, we require the probability c for getting an $\mathbf{X}_k$ such that

$$h_{\min} \leq \mathbf{a}_k^T \mathbf{X}_{k|k}^{-1} \mathbf{a}_k \leq h_{\max} \tag{57}$$

holds for all $\mathbf{a}_k$ obeying (56). As has been shown in [18], this is equivalent to having

$$h_{\max}^{-1} \leq \mathbf{a}_{k|k}^T \mathbf{X}_k^{-1} \mathbf{a}_{k|k} \leq h_{\min}^{-1} \tag{58}$$

to hold for all $\mathbf{a}_{k|k}$ that obey (55). The decisive advantage of this equivalent representation is that the marginal density of the SPD random matrix $\mathbf{X}_k$ is known.

From now on, we consider the (in a certain sense symmetric) special case $h_{\min} = 1/f$ and $h_{\max} = f$ with some factor $f = f(c) > 1$ giving the condition

$$1/f \leq \mathbf{a}_{k|k}^T \mathbf{X}_k^{-1} \mathbf{a}_{k|k} \leq f. \tag{59}$$

According to [18], this condition is fulfilled if and only if the minimum and the maximum eigenvalue of the SPD matrix

$$\mathbf{Z}_k := \left(\mathbf{X}_{k|k}^{1/2}\right)^T \mathbf{X}_k^{-1} \mathbf{X}_{k|k}^{1/2} \tag{60}$$

with $\mathbf{X}_{k|k}^{1/2}$ in analogy to (37) obey

$$\lambda_{\min}(\mathbf{Z}_k) \geq 1/f \quad \text{and} \quad \lambda_{\max}(\mathbf{Z}_k) \leq f. \tag{61}$$

But with $\mathbf{X}_k$ being distributed according to an inverse Wishart density with expected matrix $\mathbf{X}_{k|k}$ and parameter $\alpha_{k|k}$ according to (42), there holds $\mathbf{X}_k^{-1} \sim \mathcal{W}(\nu_{k|k}, \alpha_{k|k}^{-1}\mathbf{X}_{k|k}^{-1})$ and $\mathbf{Z}_k \sim \mathcal{W}(\nu_{k|k}, \alpha_{k|k}^{-1}(\mathbf{X}_{k|k}^{1/2})^T \mathbf{X}_{k|k}^{-1} \mathbf{X}_{k|k}^{1/2})$ possesses a standard

Wishart density $\mathbf{Z}_k \sim \mathcal{W}(\nu_{k|k}, \alpha_{k|k}^{-1}\mathbf{I})$. Herewith, it becomes apparent that the sought mapping between c and f does not depend on the estimate $\mathbf{X}_{k|k}$, but solely on the parameter $\alpha_{k|k} = \nu_{k|k} - d - 1$. The joint distribution of the smallest and the largest eigenvalue of $\mathbf{Z}_k$ can be obtained from a more general result in [22]. For two spatial dimensions, it reads

$$p(\lambda_{\max}, \lambda_{\min}) = \frac{\sqrt{\pi}(\lambda_{\max}\lambda_{\min})^{(\nu_{k|k}-3)/2} \cdot (\lambda_{\max} - \lambda_{\min})}{\left(\frac{2}{\alpha_{k|k}}\right)^{\nu_{k|k}} \Gamma\left(\frac{\nu_{k|k}}{2}\right) \Gamma\left(\frac{\nu_{k|k}-1}{2}\right)} \cdot \exp\left(-\frac{\alpha_{k|k}}{2}(\lambda_{\max} + \lambda_{\min})\right) \quad (62)$$

for $\lambda_{\max} \geq \lambda_{\min} \geq 0$. But, carefully using some partial integration, we can solve the double integral

$$\begin{aligned} c(f) &= P\{1/f \leq \lambda_{\min} \wedge \lambda_{\max} \leq f\} \\ &= \int_{1/f}^{f} \int_{1/f}^{\lambda_{\max}} p(\lambda_{\max}, \lambda_{\min}) \mathrm{d}\lambda_{\min} \mathrm{d}\lambda_{\max} \end{aligned} \quad (63)$$

and obtain

$$c(f) = \Gamma(2\beta, 2\Lambda_2) - \Gamma(2\beta, 2\Lambda_1) - \sqrt{\pi}\frac{e^{-\Lambda_1}\Lambda_1^{\beta} + e^{-\Lambda_2}\Lambda_2^{\beta}}{\Gamma\left(\beta + \frac{1}{2}\right)} \cdot (\Gamma(\beta, \Lambda_2) - \Gamma(\beta, \Lambda_1)) \quad (64)$$

with the abbreviations

$$\Lambda_1 := \frac{\alpha_{k|k}}{2f} \qquad \Lambda_2 := \frac{\alpha_{k|k} f}{2} \qquad \beta := \frac{\alpha_{k|k}}{2} + 1 \quad (65)$$

and the normalized incomplete gamma function $\Gamma(t, x) = (1/\Gamma(t)) \int_0^x e^{-\xi}\xi^{t-1}\mathrm{d}\xi$. The function $c(f)$ in (63) obviously is strictly increasing and thus invertible, the sought mapping $f(c)$ is easily obtained from $c(f)$ for any given confidence c by standard means.

V. IMM

Multiple model approaches like the interacting multiple model (IMM) are well-known candidates for significantly improving overall tracking performance if targets may switch between maneuvering and non-maneuvering behavior. Details about the IMM for point targets can be found at various places in literature, e.g., in [23]. Now, our approach of Section III can be integrated in an IMM framework with a suitable adjustment of some steps using a set of R models with different process noises and extension agility time constants.

Denoting by $\pi_{k-1|k-1}^{i}$ the probability of model i having been true at scan $k-1$ and by π^{ij} the probability of transitioning from model i to model j, the processing cycle starts with the computation of the predicted model probabilities[2]

$$\pi_{k|k-1}^{j} = P\{\pi_k = j | \boldsymbol{\mathcal{Y}}_{k-1}\} = \sum_{i=1}^{R} \pi^{ij}\pi_{k-1|k-1}^{i} \quad (66)$$

and the mixing probabilities $P\{\pi_{k-1} = i | \pi_k = j, \boldsymbol{\mathcal{Y}}_{k-1}\}$, i.e.,

$$\pi_{k-1|k-1}^{i|j} = \pi^{ij}\pi_{k-1|k-1}^{i}/\pi_{k|k-1}^{j}. \quad (67)$$

[2]The random variable π_k indicates the dynamic model, which is in effect throughout the prediction step from scan $k-1$ to scan k.

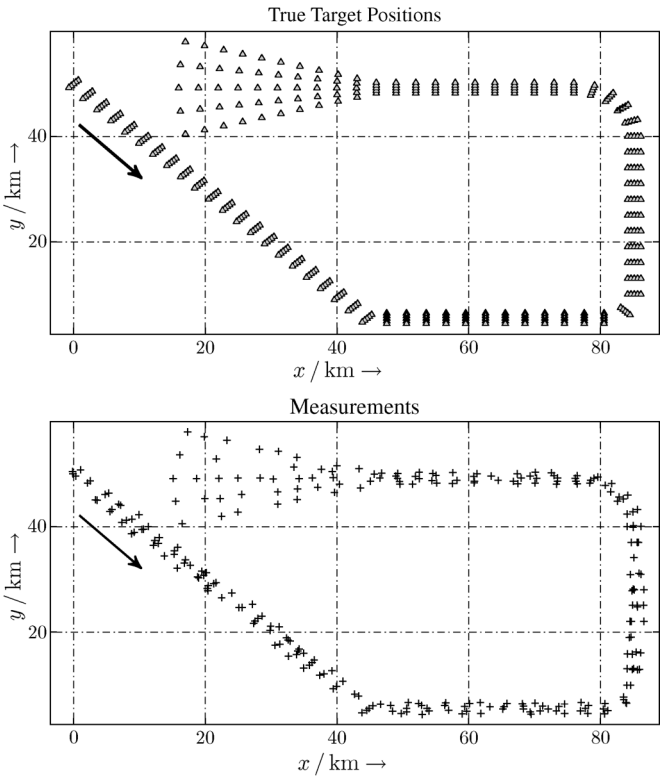

Fig. 4. Group tracking scenario with 5 targets. Shown are, for each time t_k, the true target positions (top) as well as the measurements (bottom).

With these, we perform the standard interaction step

$$\mathbf{x}_{k-1|k-1}^{0j} = \sum_{i=1}^{R} \pi_{k-1|k-1}^{i|j} \mathbf{x}_{k-1|k-1}^{i} \quad (68)$$

$$\mathbf{P}_{k-1|k-1}^{0j} = \sum_{i=1}^{R} \pi_{k-1|k-1}^{i|j} \left(\mathbf{P}_{k-1|k-1}^{i} + \left(\mathbf{x}_{k-1|k-1}^{i} - \mathbf{x}_{k-1|k-1}^{0j}\right) \times \left(\mathbf{x}_{k-1|k-1}^{i} - \mathbf{x}_{k-1|k-1}^{0j}\right)^{T}\right) \quad (69)$$

for the centroid kinematics estimate. This step can be motivated by replacing the true resulting (in our case marginal) Gaussian mixture densities by normal densities with the same first and second order moments. As has been mentioned in Section IV-B, a corresponding matching of the second order moments cannot be fully done for the inverse Wishart densities that describe the extension. Yet, in view of the results above, a complete first order moment matching in combination with the scalar second order moment matching yields

$$\mathbf{X}_{k-1|k-1}^{0j} = \sum_{i=1}^{R} \pi_{k-1|k-1}^{i|j} \mathbf{X}_{k-1|k-1}^{i} \quad (70)$$

$$e_{k-1|k-1}^{0j} = \sum_{i=1}^{R} \pi_{k-1|k-1}^{i|j} \times \left(e_{k-1|k-1}^{i} + \mathrm{tr}\left(\left(\mathbf{X}_{k-1|k-1}^{i} - \mathbf{X}_{k-1|k-1}^{0j}\right)^2\right)\right) \quad (71)$$

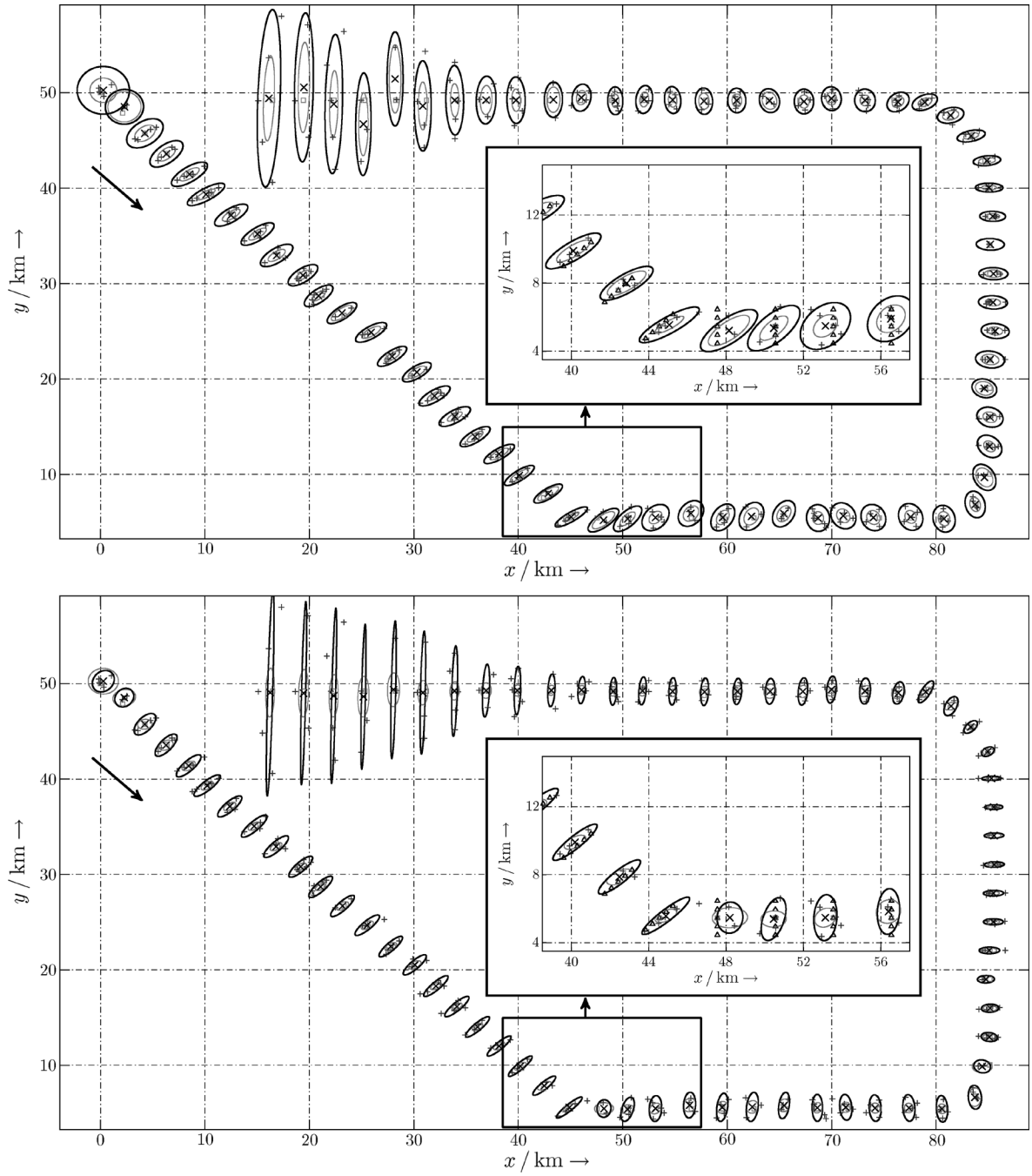

Fig. 5. Tracking results for the sensor data of Fig. 4. Used were the original approach as presented in Section II (top) and our new group tracking algorithm using an IMM with three models (bottom). Shown are, for each time t_k, the true target positions ($\triangle$), the true centroid ($\square$), the measurements ($+$), the (updated) estimated centroid ($\times$) with the corresponding 90%-confidence ellipse (thin line), as well as the (updated) estimated group extension (thick line).

so that, with (51) in mind, we can obtain $\alpha^{0j}_{k-1|k-1}$. Starting from these initial values, each model is individually updated with the measurements.

In order to proceed further, the model-dependent measurement likelihoods $\Lambda^j_{k|k-1} = p(\mathbf{Y}_k|\pi_k = j, \mathcal{Y}_{k-1})$ have to be computed next. Again, these are not known exactly. At this point, we choose a somewhat heuristic procedure that does not only take into account the innovation likelihood of the mean measurement with respect to the centroid but also how well the measurement spread matches the predicted extension. Bearing in mind the scaling factor z for object extension (see Section III-A), we introduce

$$\begin{aligned}\Delta^j_{k|k-1} &:= \overline{\mathbf{Y}}_k - (n_k - 1)\mathbf{Y}^j_{k|k-1} \\ &:= \Delta\mathbf{Y}^j_k + z(n_k - 1)\left(\mathbf{X}_k - \mathbf{X}^j_{k|k-1}\right) \qquad (72)\end{aligned}$$

$$\text{with} \quad \Delta\mathbf{Y}^j_k := \overline{\mathbf{Y}}_k - (n_k - 1)(z\mathbf{X}_k + \mathbf{R}) \qquad (73)$$

and $\mathbf{Y}^j_{k|k-1} = z\mathbf{X}^j_{k|k-1} + \mathbf{R}$ as the model-specific predicted variance of a single measurement in analogy to (33). Due to

$E[\Delta\mathbf{Y}_k^j] = \mathbf{0}$, the variance of $\Delta\mathbf{Y}_k^j$ for given $\mathbf{X}_k$ can be obtained from the Wishart density $\mathcal{W}(\overline{\mathbf{Y}}_k; n_k - 1, z\mathbf{X}_k + \mathbf{R})$, which is equal to the matrix-variate part of our measurement likelihood function. Therefore, we use a result in [19] that, replacing $\mathbf{X}_k$ with the model-specific prediction $\mathbf{X}_{k|k-1}^j$ afterwards, approximately is[3]

$$\mathrm{Var}\left[\Delta\mathbf{Y}_k^j\right] \approx (n_k - 1)\left(\mathrm{tr}\left(\mathbf{Y}_{k|k-1}^j\right)\mathbf{Y}_{k|k-1}^j + \left(\mathbf{Y}_{k|k-1}^j\right)^2\right). \tag{74}$$

With model-specific $\mathbf{V}_{k|k-1}^j$ given as in (50) and in view of

$$\mathrm{Var}\left[\Delta_{k|k-1}^j\right] \approx \mathrm{Var}\left[\Delta\mathbf{Y}_k^j\right] + z^2(n_k - 1)^2\mathbf{V}_{k|k-1}^j \tag{75}$$

we propose to use

$$\Lambda_{k|k-1}^j \propto \mathcal{N}\left(\overline{\mathbf{y}}_k; \mathbf{H}\mathbf{x}_{k|k-1}^j, \mathbf{S}_{k|k-1}^j\right) \times \left|2\pi\mathrm{Var}\left[\Delta_{k|k-1}^j\right]\right|^{-\frac{d+1}{4}} \cdot \mathrm{etr}\left(-\frac{1}{2}\Delta_{k|k-1}^j\left(\mathrm{Var}\left[\Delta_{k|k-1}^j\right]\right)^{-1}\Delta_{k|k-1}^j\right) \tag{76}$$

for $n_k \geq 2$ and solely $\Lambda_{k|k-1}^j \approx \mathcal{N}(\overline{\mathbf{y}}_k; \mathbf{H}\mathbf{x}_{k|k-1}^j, \mathbf{S}_{k|k-1}^j)$ in case of a single measurement. Now, we obtain the updated model likelihoods according to

$$\pi_{k|k}^j = P\{\pi_k = j|\mathcal{Y}_k\} = \frac{\Lambda_{k|k-1}^j \pi_{k|k-1}^j}{\sum_{i=1}^R \Lambda_{k|k-1}^i \pi_{k|k-1}^i} \tag{77}$$

before finally computing, for output purposes only, the mixed estimates from the updated model estimates in analogy to the interaction step from (68)–(71) with, among other things, $\pi_{k-1|k-1}^{i|j}$ replaced by $\pi_{k|k}^j$.

VI. Simulation Results

A. Group Tracking Scenario

For comparing both tracking approaches as presented in Sections II and III, we have simulated a formation of 5 individual targets flying with constant speed $v = 300$ m/s in the (x, y)-plane. The targets were arranged in a line with 500 m distance between neighboring targets, where the formation first went through a 45° and two 90° turns (with radial accelerations 2 g, 2 g, and 1 g, respectively) before performing a split-off maneuver. This formation was observed by a (fictitious) sensor with scan time $T = 10$ s delivering uncorrelated x- and y-measurements with standard deviations $\sigma_x = 500$ m and $\sigma_y = 100$ m, respectively, where we assumed a probability of detection $P_\mathrm{d} = 80\%$ for each target (instead of a detailed model for limited sensor resolution). With this, the true joint measurement likelihood is a Gaussian mixture and (2) as well as (28) can only be (good or bad) approximations thereof.

The top part of Fig. 5 shows the tracking results of the original algorithm of [13]. We have used a constant velocity dynamic model, where the process noise term $\widetilde{\mathbf{Q}}$ was chosen according to a white acceleration model [23] and tuned in such a way that the estimator was (just) able to follow the 2 g turns. In the bottom part of Fig. 5, we have applied an IMM variant of our new group tracking approach to the same simulated data. The IMM consisted of three white acceleration models for the kinematics,

[3]Let $\mathbf{X} \sim \mathcal{W}(m, \mathbf{C})$ according to the parameterization (5), then it yields $E[\mathbf{X}^2] = m\mathbf{C}^2 + m\mathrm{tr}(\mathbf{C})\mathbf{C} + m^2\mathbf{C}^2$, i.e., $\mathrm{Var}[\mathbf{X}] = m\mathbf{C}^2 + m\mathrm{tr}(\mathbf{C})\mathbf{C}$.

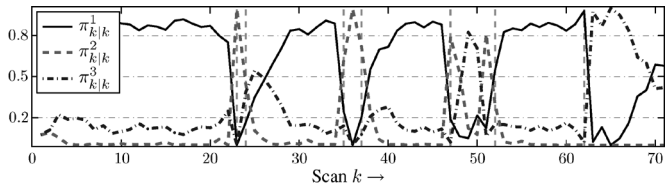

Fig. 6. Model probabilities after update for the algorithm of Fig. 5 (bottom). The IMM consisted of a low-noise model (solid line), a high-noise model with very high extension agility (dashed line), and a model with moderate process noise and high extension agility (dot and dash line).

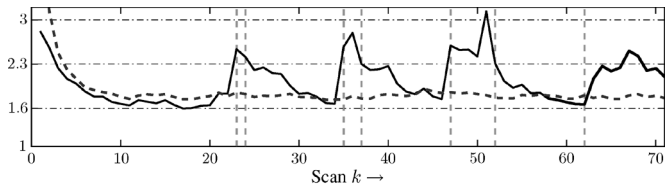

Fig. 7. Scaling factors $f_{k|k}$ to obtain the confidence regions ($c = 70\%$) of the (updated) estimated group extension for the original approach as presented in Section II (dashed line) and our new group tracking algorithm using an IMM with three models (solid line).

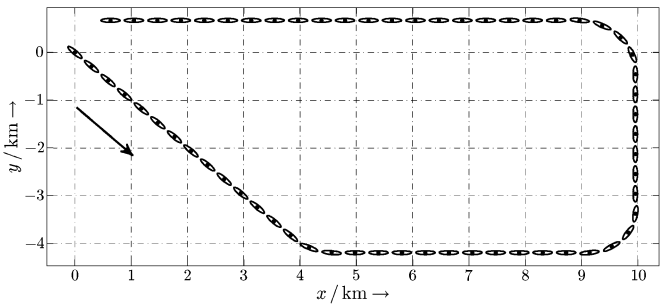

Fig. 8. Trajectory of an extended target. Shown are, for every third scan k, the true centroid positions as well as the true physical object extensions.

where we have combined a low kinematic process noise with a low extension agility, a high kinematic process noise with some very high extension agility—this model accounts for possibly rapid changes of shape, size, and (absolute) orientation during maneuvers that may be initiated by some lead target—plus a third model with moderate kinematic process noise and high extension agility covering extension changes of formations that do not maneuver too much. In comparison with the original approach, we have to notice a significant improvement using the new algorithm. It adopts much faster to the orientation changes after the maneuvers while showing smoother centroid position estimates in the non-maneuvering phases of the flight. During split-off, it reacts by far less sensitive to missed detections. In addition, we see that the new approach can indeed still compensate the sensor error to a large extent and thus, although compensation is not complete, is able to detect the orientation change. Finally, we note that the position estimation error no longer equals the estimated extension up to a scalar factor. Fig. 6 shows how the individual model probabilities vary over time. The high-noise model responds to rapid changes of the centroid kinematics. After the maneuvers have finished (as well as in the middle of the more shallow 1 g maneuver), the model adapted to extent changes exhibits some increased contributions before the low-noise model takes over again after adjustment of the orientation. And, the former model is dominant in the split-off phase,

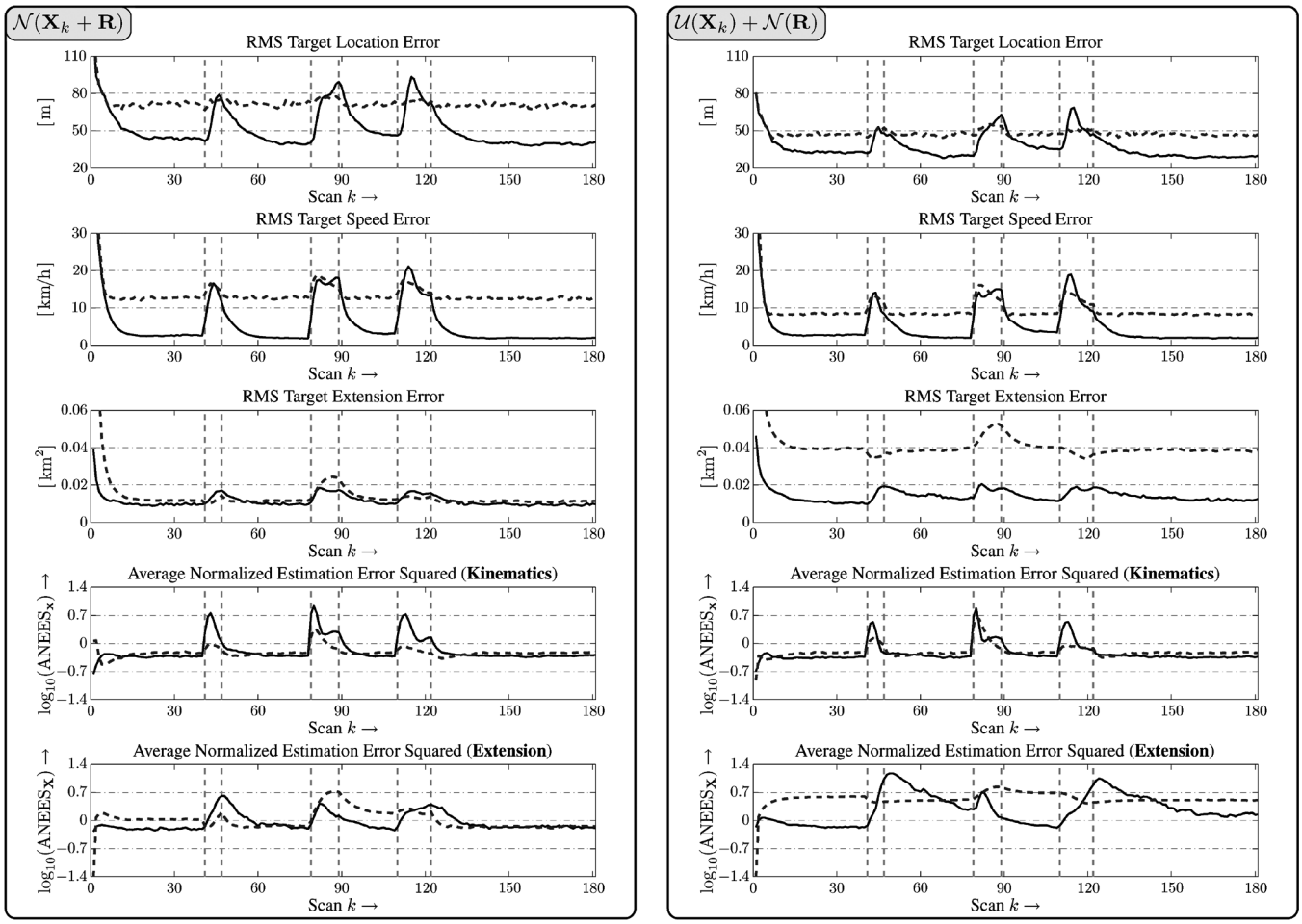

Fig. 9. Simulation results of 900 Monte Carlo runs for both measurement generating models, i.e., the left part summarizes the results of $\mathcal{N}(\mathbf{X}_k + \mathbf{R})$ and, accordingly, the right part the results of $\mathcal{U}(\mathbf{X}_k) + \mathcal{N}(\mathbf{R})$. Shown are absolute and relative errors to compare the original approach as presented in Section II (dashed line) with our extended object tracking algorithm using an IMM with three models (solid line).

where the centroid does not show any significant maneuvering behavior but the extent of the formation changes rapidly.

Fig. 7 wraps up this scenario by plotting the values $f = f_{k|k}$ of (64) for both tracking algorithms: the greater this value and herewith the confidence region for a specific estimated extension is, the less reliable the estimate is considered. While the values of the new approach indicate a decreased reliability during and just after maneuvering phases (as can be expected), the ones of the original algorithm level off at almost a constant value. This peculiarity motivates some more detailed investigation of the self-assessment of the two estimators regarding their estimation errors for both kinematics and extension.

B. Extended Object Scenario

When using estimators, credibility of estimates is an important quality measure in addition to MSE and confidence regions. Here, we exploit, with $d_{k|k}$ according to (54), the average normalized estimation error squared

$$\text{ANEES}_\mathbf{x} = \frac{1}{M \dim(\mathbf{x}_k)} \sum_{\mu=1}^{M} \left[d_{k|k} \right]_\mu \tag{78}$$

where the subscript μ indicates tracking results concerning the μth run of a Monte Carlo simulation totaling M runs. In order to transfer this credibility measure to the extension estimate, we normalize the sum of the mean square errors obtained for each matrix element by $e_{k|k} = \text{tr}\mathbf{V}_{k|k}$ of (50) ending up with

$$\text{ANEES}_\mathbf{X} = \frac{1}{M} \sum_{\mu=1}^{M} \left[\frac{\text{tr}\left[(\mathbf{X}_{k|k} - \mathbf{X}_k)^2 \right]}{e_{k|k}} \right]_\mu . \tag{79}$$

For both types of ANEES, values larger than 1 indicate that the filter is overly confident about its estimation quality. In addition to the known relative $(\text{ANEES}_\mathbf{x}, \text{ANEES}_\mathbf{X})$ and absolute errors, i.e., target location error (TLE) and target speed error (TSE), we regard

$$\text{RMSE}_\mathbf{X} = \sqrt{\frac{1}{M} \sum_{\mu=1}^{M} \left[\text{tr}\left[(\mathbf{X}_{k|k} - \mathbf{X}_k)^2 \right] \right]_\mu} \tag{80}$$

as the root mean square target extension error.

Of course, $\text{ANEES}_\mathbf{X}$ and $\text{RMSE}_\mathbf{X}$ can only be computed if there exists some type of true $\mathbf{X}_k$. For this reason, we have considered an ellipse with diameters 340 and 80 m (about the size of an aircraft carrier of the Nimitz-class) as an extended object in the (x, y)-plane following the target trajectory in Fig. 8, where the speed was assumed to be constant at 27 knots (≈50 km/h). In addition to a model generating measurements according to the measurement likelihood $\mathbf{y}_k^j \sim \mathcal{N}(\mathbf{H}\mathbf{x}_k, \mathbf{X}_k + \mathbf{R})$, a second model has been used that follows our comment in Section III-A

and assumes that scattering centers are uniformly distributed over the extension $\mathbf{X}_k$ while measurements are subject to a zero-mean Gaussian noise with variance $\mathbf{R}$. The number of measurements in each scan generated by the two models was Poisson-distributed with mean 5. Sensor parameters were $\sigma_x = 100$ m and $\sigma_y = 20$ m with scan time $T = 10$ s. For the first model, hereinafter referred to as $\mathcal{N}(\mathbf{X}_k + \mathbf{R})$, a scaling factor $z = 1$ was used and $z = 1/4$ for the second, $\mathcal{U}(\mathbf{X}_k) + \mathcal{N}(\mathbf{R})$.

The results of Monte Carlo simulations with $M = 900$ runs each are summarized in Fig. 9. The improvement of the new algorithm when compared to the original one regarding TLE and TSE for both measurement generating models is immediately apparent (apart from some peaks during maneuver onset that are typical for an IMM). The overestimation of the extension as expected for the original approach manifests in some increased target extension error (TXE) during non-maneuver phases for the measurement model $\mathcal{N}(\mathbf{X}_k+\mathbf{R})$ and, amplified, throughout the scenario for $\mathcal{U}(\mathbf{X}_k)+\mathcal{N}(\mathbf{R})$. With respect to the self assessment of the estimators (shown by logarithms of the ANEES for kinematics and extension), the situation is not quite as clear cut. Both approaches appear to be too optimistic about their kinematic estimates for some time after maneuver onset (again, typical for an IMM) and too pessimistic during remaining non-maneuver phases with the new approach showing this more than the original one. The results for the extension leave room for further discussion.

VII. Conclusion

The focus of this paper was on some recently published approaches to tracking of extended objects and group targets delivering more than one measurement per scan. The novelty of these approaches relies on modeling the extent by means of an SPD random matrix. We have proposed a way to modify a previously published approach that originally has been derived as a closed form solution to the Bayesian estimation problem under the simplifying assumption of neglectable sensor error. With careful adoptions, a new approach has evolved that can easily be used within an IMM framework and that yields improved performance for cases where sensor errors, when compared with object extension, cannot be neglected any more. Further related aspects and properties of extension estimation based on SPD matrices have been discussed.

Future work certainly must include the estimation of target numbers within a formation plus, surely the most challenging task, the derivation of sophisticated data association techniques. In this context, the estimation error variance of the extension part will play a decisive role in future developments, e.g., for gating and scoring. This raises the interesting (but not yet answerable) question of what an acceptable estimation error is, when there is no real ellipsoidal extension $\mathbf{X}_k$ (e.g., for aircraft formations, convoys, etc.).

References

[1] J. Dezert, "Tracking maneuvering and bending extended target in cluttered environment," in *Proc. SPIE Conf. Signal Data Process. Small Targets*, O. E. Drummond, Ed., Orlando, FL, 1998, vol. 3373, pp. 283–294.

[2] F. E. Daum and R. J. Fitzgerald, "Importance of resolution in multiple-target tracking," in *Proc. SPIE Conf. Signal Data Process. Small Targets*, Orlando, FL, 1994, vol. 2235, pp. 329–338.

[3] S. S. Blackman and R. Popoli, *Design and Analysis of Modern Tracking Systems*. Norwood, MA: Artech House, 1999.

[4] W. Koch and G. van Keuk, "Multiple hypothesis track maintenance with possibly unresolved measurements," *IEEE Trans. Aerosp. Electron. Syst.*, vol. 33, no. 3, pp. 883–892, 1997.

[5] S. Gadaleta, A. B. Poore, S. Roberts, and B. J. Slocumb, "Multiple hypothesis clustering, multiple frame assignment, tracking," in *Proc. SPIE Conf. Signal Data Process. Small Targets*, O. E. Drummond, Ed., Orlando, FL, 2004, vol. 5428, pp. 294–307.

[6] D. Clark and S. Godsill, "Group target tracking with the Gaussian mixture probability hypothesis density filter," in *Proc. Int. Conf. Intell. Sensors, Sensor Netw., Inform.*, Melbourne, Australia, 2007, pp. 149–154.

[7] S. K. Pang, J. Li, and S. J. Godsill, "Models and algorithms for detection and tracking of coordinated groups," in *Proc. IEEE Aerospace Conf.*, Big Sky, MT, 2008, 17 pages.

[8] K. Gilholm, S. Godsill, S. Maskell, and D. Salmond, "Poisson models for extended target and group tracking," in *Proc. SPIE Conf. Signal Data Process. Small Targets*, San Diego, CA, 2005, vol. 5913, 12 pages.

[9] K. Gilholm and D. Salmond, "Spatial distribution model for tracking extended objects," *IEE Radar Sonar Navig.*, vol. 152, no. 5, pp. 364–371, 2005.

[10] B.-T. Vo, B.-N. Vo, and A. Cantoni, "Bayesian filtering with random finite set observations," *IEEE Trans. Signal Process.*, vol. 56, no. 4, pp. 1313–1326, Apr. 2008.

[11] M. Baum and U. D. Hanebeck, "Extended object tracking based on combined set-theoretic and stochastic fusion," in *Proc. Int. Conf. Inform. Fusion*, Seattle, WA, 2009, pp. 1288–1295.

[12] M. J. Waxman and O. E. Drummond, "A bibliography of cluster (group) tracking," in *Proc. SPIE Conf. Signal Data Process. Small Targets*, O.E. Drummond, Ed., Orlando, FL, 2004, vol. 5428, pp. 551–560.

[13] W. Koch, "Bayesian approach to extended object and cluster tracking using random matrices," *IEEE Trans. Aerosp. Electron. Syst.*, vol. 44, no. 3, pp. 1042–1059, 2008.

[14] S. S. Blackman, *Multiple-Target Tracking With Radar Applications*. Norwood, MA: Artech House, 1986.

[15] O. E. Drummond, S. S. Blackman, and G. C. Petrisor, "Tracking clusters and extended objects with multiple sensors," in *Proc. SPIE Conf. Signal Data Process. Small Targets*, O.E. Drummond, Ed., Orlando, FL, 1990, vol. 1305, pp. 362–375.

[16] D. J. Salmond and M. C. Parr, "Track maintenance using measurements of target extent," *IEE Radar, Sonar, Navig.*, vol. 150, no. 6, pp. 389–395, 2003.

[17] M. Feldmann and D. Fränken, "Tracking of extended objects and group targets using random matrices—A new approach," in *Proc. Int. Conf. Inform. Fusion*, Cologne, Germany, 2008, pp. 242–249.

[18] M. Feldmann and D. Fränken, "Advances on tracking of extended objects and group targets using random matrices," in *Proc. Int. Conf. Inform. Fusion*, Seattle, WA, 2009, pp. 1029–1036.

[19] A. K. Gupta and D. K. Nagar, *Matrix Variate Distributions*. Boca Raton, FL: Chapman & Hall/CRC Press, 1999.

[20] D. A. Harville, *Matrix Algebra From a Statistician's Perspective*. New York: Springer-Verlag, 1997.

[21] S. Kotz and S. Nadarajah, *Multivariate t-Distributions and Their Applications*. Cambridge, U.K.: Cambridge Univ. Press, 2004.

[22] R. J. Muirhead, *Aspects of Multivariate Statistical Theory*. New York: Wiley, 1982.

[23] Y. Bar-Shalom, X. R. Li, and T. Kirubarajan, *Estimation With Applications to Tracking and Navigation (Theory, Algorithms and Software)*. New York: Wiley, 2001.

Michael Feldmann received the B.Sc. and M.Sc. degrees in electrical engineering from the University of Paderborn, Germany, in 2006 and 2007, respectively.

Since 2007, he has been working in the Sensor Data and Information Fusion Department, Fraunhofer Institute for Communication, Information Processing and Ergonomics FKIE, Wachtberg, Germany. He is also member of the Ph.D. graduation program (Prof. Hanebeck) at the Karlsruhe Institute of Technology, Germany. His research interests include tracking of extended objects and group targets.

Dietrich Fränken (M'89) received the Dipl.-Ing. degree in electrical engineering from the Ruhr-Universität Bochum, Germany, in 1991 and the Dr.-Ing. and Dr.-Ing. habil. degrees from the University of Paderborn, Germany, in 1997 and 2003, respectively.

Currently, he is a Research Development and Systems Engineer within the Data Fusion Algorithms and Software Department of Cassidian, an EADS company, Ulm, Germany, where he is heading the future systems and technologies group. Simultaneously, he is giving lectures on synthesis and design of digital filters at the University of Ulm, Germany. His research interests include modeling, simulation, and estimation of physical systems, nonlinear filtering, graph and system theory, and digital signal processing.

Wolfgang Koch (M'97–SM'09–F'11) studied mathematics and physics and received the Ph.D. degree from the Aachen Technical University, Aachen, Germany, in 1990.

At present, he is head of the Sensor Data and Information Fusion Department, Fraunhofer Institute for Communication, Information Processing and Ergonomics FKIE, Wachtberg, Germany. He regularly gives lectures related to sensor data fusion at Bonn University, Institute of Computer Science. His current research interests are related to statistical estimation theory, multiple data sensor fusion, multiple target tracking, sensor management, ground surveillance, passive surveillance, multistatic tracking, and sensor data/information fusion in general. On this area, he has published several book chapters and numerous journal and conference papers.

Dr. Koch is Technical Editor for *Target Tracking and Multisensor Systems* and the IEEE TRANSACTIONS ON AEROSPACE AND ELECTRONIC SYSTEMS. Together with P. Willett, University of Connecticut, Storrs, he was Co-Chairman of FUSION 2008.